

The effect of energy weighting on the SNR under the influence of non-ideal detectors in mammographic applications

G. Patatoukas^a, A. Gaitanis^{a,b}, N. Kalivas^c, P. Liaparinos^{a,b}, D. Nikolopoulos^b,
A. Konstantinidis^b, I. Kandarakis^{b,*}, D. Cavouras^b, G. Panayiotakis^a

^aLaboratory of Medical Physics, Medical School, University of Patras, 26500 Patras, Greece

^bDepartment of Medical Instruments Technology, Technological Educational Institute of Athens, Agion Spyridonos Street, Egaleo, 12210 Athens, Greece

^cGreek Atomic Energy Commission, 15310 Ag. Paraskevi, P.O. box 60092, Greece

Available online 1 September 2006

Abstract

This work investigates the effect of the energy-weighting technique on the signal to noise ratio (SNR) response of X-ray imaging detectors. So far in the literature all scintillation-detector characteristics (detection efficiency, conversion efficiency, light-attenuation effects, etc) that degrade image quality have been ignored. A theoretical evaluation of the scintillator's SNR output was carried out. An algorithm was produced to describe the variation of the weighting factor, and SNR, with respect to the anode material (Mo or W), in a particular energy range (25–40 keV), typical for mammography, using two different phantoms. Results show that under non-ideal conditions the ratio of the weighted SNR to the original SNR appears to be increasing from values that are close to unity, and under specific conditions, can reach values up to 30. For the further investigation of this method, a more complex, simulated computed tomography breast imaging system was modeled and studied for various parameters such as breast software phantoms, scintillation materials and reconstruction filters.

© 2006 Elsevier B.V. All rights reserved.

PACS: 07.85; 78.65; 42.80

Keywords: SNR; Energy weighting; Scintillators; X-ray mammography; Breast CT

1. Introduction

The idea of signal enhancement with the use of an energy-dependent function that operates upon the detector's output signal has already been considered as a promising technique [1,2]. With the application of this method, the signal to noise ratio (SNR) and other parameters (DQE, contrast etc.) could see an improvement that could help the diagnostic procedure.

Such concept has been previously reported in the literature in two cases [1,2]. In both these studies all noise sources have been assumed to be zero except for quantum fluctuations. Monte Carlo simulation showed that energy weighting resulted in SNR enhancement by a factor of 1.9 [2]. In addition, such an SNR enhancement is more

obvious when using molybdenum anode rather than tungsten anode [1]. Finally, it has been reported that DQE results, for weighted signals, were similar for microcalcification regions and tumors [2].

The present study investigates how an energy-dependent weighting function affects the SNR in the presence of a non-ideal scintillation detector under mammographic conditions. An algorithm was produced to study the variation of the weighting factor in terms of anode material and in terms of tumor or microcalcification thickness. Furthermore, to justify the effect of this method on image quality, a computed tomography breast imaging (CTBI) system was simulated. In this model not only the effect of energy-weighted technique was studied but also other parameters such as detector scintillation materials and their properties (quantum detection efficiency, intrinsic efficiency, detector optical gain, etc.) were taken into consideration.

*Corresponding author. Tel.: +30 210 5385 375; fax: +30 210 5910 975.
E-mail address: kandarakis@teiath.gr (I. Kandarakis).

2. Materials and methods

2.1. Definition of energy weighting

A typical X-ray situation is shown in Fig. 1. Under these conditions the energy weighting factor was defined in the following way [2]:

$$W = \frac{S_1 - S_2}{S_1 + S_2}, \quad (1)$$

where S_1 and S_2 are the signals corresponding to different regions of the phantom, as seen in Fig. 1.

2.2. Simulation set up

To simulate the complete imaging situation, different anode materials (molybdenum and tungsten) were used for a variety of different energies from 25 to 40 kV. All spectra were downloaded from the SIEMENS website [4] and were created according to a previously published algorithm [5]. The phantom designed was one-dimensional and can be seen in Fig. 1. It included breast tissue of thickness 4.5 cm and tumor (or microcalcification) of varying thickness. Attenuation coefficient values for breast, microcalcification and tumor were calculated according to the following formulae according to Cahn et al. [1]:

$$\tau(E) = 24.15Z^{4.2}E^{-3} + 0.56Z, \quad (2)$$

$$\mu(E) = \frac{\tau(E)\rho N_0}{A}, \quad (3)$$

where τ is the cross-section, Z is the atomic number, E is the X-ray photon energy, ρ is the material density, A is the atomic mass and N_0 is the Avogadro's number. Values for these parameters were obtained by Cahn et al. [1].

The detector considered in the present study was based on a $\text{Gd}_2\text{O}_2\text{S:Tb}$ screen with a coating thickness of 31.7 mg/cm^2 typically used for mammographic examinations. The emission for this material exhibits the highest intensity spectral line at 545 nm, in the green region of the spectrum. Its density is 7.3 g/cm^3 , it is not hydroscopic and its decay time is of order of 10^6 ns [3].

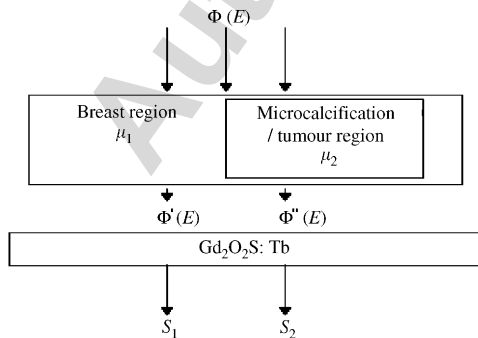


Fig. 1. Typical X-ray imaging situation using a phantom with two different regions (breast and microcalcification, or breast and tumor).

An important parameter that characterizes a scintillation screen is the function \bar{g}_λ . This parameter represents the fraction of light flux generated in the phosphor material at depth t and transmitted to the screen output, giving the final signal. The full expression for \bar{g}_λ is given by Eq. (4), as previously published [6–9]

$$\bar{g}_\lambda(t) = \frac{\tau\rho_i[(\tau\rho_o + \sigma)e^{\sigma t} + (\sigma - \tau\rho_o)e^{-\sigma t}]}{(\tau\rho_o + \sigma)(\tau\rho_i + \sigma)e^{\sigma T} - (\sigma - \tau\rho_o)(\sigma - \tau\rho_i)e^{-\sigma T}}, \quad (4)$$

where $\tau = \sigma/\beta$ and σ , β are optical parameters, t is the scintillator's depth where the light flux was generated, and T is the total coating thickness of the detector. For $\text{Gd}_2\text{O}_2\text{S:Tb}$, the following values were assigned to the three parameters: $\sigma = 30$, $\beta = 0.03$ and ρ characterizes the reflectivity of the inner surface of the phosphor at either the input, ρ_i , or the output ρ_o [9].

3. Signal and noise definition

For the calculation of the scintillator's output signal the following formulae were used [10]:

$$S_1 = \int_E \int_T \Phi'_0(E) e^{-\mu t} \mu \eta_c \frac{E}{E_\lambda} \bar{g}_\lambda(t) dE dt, \quad (5)$$

$$S_2 = \int_E \int_T \Phi''_0(E) e^{-\mu t} \mu \eta_c \frac{E}{E_\lambda} \bar{g}_\lambda(t) dE dt. \quad (6)$$

In the above expressions S_1 denotes the signal exiting the scintillator that has passed from the breast region, and S_2 denotes the signal that has passed from both regions; $\Phi'_0(E)$, $\Phi''_0(E)$ are the signals coming out the breast region and the breast microcalcification/tumor region, respectively. η_c is the intrinsic conversion efficiency, expressing the fraction of the absorbed radiation energy that is converted into light within the scintillator mass, E is the energy of the X-ray photon, E_λ is the optical photon energy, T is the total scintillator thickness, μ is the detector's attenuation coefficient. η_c was set equal to 0.19 and E_λ was set equal to 2.4 eV [9].

In a similar way, quantum noise for both signals was defined according to the variance of the signal, giving

$$N_1 = \int_E \int_T \Phi'_0(E) e^{-\mu t} \mu \left[\eta_c \frac{E}{E_\lambda} \bar{g}_\lambda(t) \right]^2 dE dt, \quad (7)$$

$$N_2 = \int_E \int_T \Phi''_0(E) e^{-\mu t} \mu \left[\eta_c \frac{E}{E_\lambda} \bar{g}_\lambda(t) \right]^2 dE dt, \quad (8)$$

for the two signals. The signal to noise ratio was calculated to be equal to Eq. (9):

$$\text{SNR} = \frac{S_1 - S_2}{(N_1 + N_2)^{1/2}}. \quad (9)$$

Finally, the weighted SNR was defined as follows

$$\text{SNR}_{\text{weighted}} = \frac{[(S_1 - S_2)W^2]}{[(N_1 + N_2)W^2]^{1/2}}. \quad (10)$$

Concluding, a new variable can be defined using Eqs. (9) and (10), namely the $\text{SNR}_{\text{ratio}}$.

$$\text{SNR}_{\text{ratio}} = \frac{\text{SNR}_{\text{weighted}}}{\text{SNR}} \quad (11)$$

4. Further simulations

To further investigate the energy-weighting technique, a CTBI system was simulated. The studied CTBI system consisted of the following parts: (a) an X-ray tube producing a poly-energetic parallel beam with tube voltages ranging from 20 to 40 kV. As cathode and filter material molybdenum cathode and molybdenum filter with thickness of 30 μm (Mo/Mo) were simulated, (b) a scintillator-based energy-weighted detector array obtaining Two-dimensional images and (c) the image-reconstruction software.

In the simulation process, further modeling of a detector was performed in order to investigate if the energy-weighting method can be affected by other parameters, such as the detector material and thickness. For this reason data from different detector materials were studied. These materials were CsI:Tl, $\text{Gd}_2\text{O}_2\text{S:Pr}$ (UFC) or GOS, $\text{Y}_3\text{Al}_5\text{O}_{12}:\text{Ce}$ (YAG), $\text{YAlO}_3:\text{Ce}$ (YAP), $\text{Y}_{1.34}\text{Gd}_{0.60}\text{O}_3:(\text{Eu,Pr})_{0.06}$ (brand name Hilight or YGO) and CdWO_4 at the thickness of 1000 mg/cm^2 . Also, the detector array was modeled as a three-stage system, including the X-ray absorption (QDE), the X-ray into light conversion and the light transmission [11]. For the evaluation of the reconstructed image two different software phantoms were created based on previous works [12]. Image reconstruction was performed using the filtered back-projection (FBP) algorithm and five different reconstruction filters. These filters were the Shepp–Logan, the Ram–Lak, the Cosine, the Hamming and the Hanning. During the simulation two different kind of sinograms (weighted and non-weighted) were created for every studied scintillator material.

5. Results and discussion

Results of the one-dimensional simulation are shown in Figs. 2 and 3. Fig. 2 shows the SNR ratio variation with microcalcification thickness at 30 keV and Fig. 3 shows the SNR ratio variation with tumor thickness at 30 keV for the two anode materials. In both cases the SNR enhancement is obvious. In the first case, the larger the size of the microcalcification, the higher the SNR ratio becomes, with values that reach 30.9 when the microcalcification size is 0.2 cm. When using Mo anode instead of W, under the same conditions (same energy, same lesion size), the

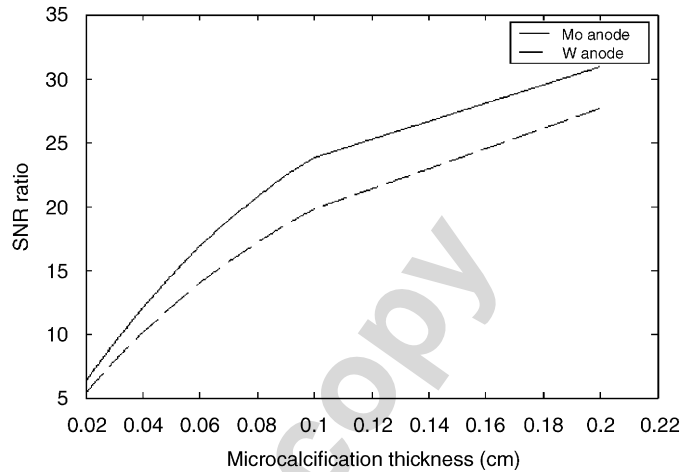


Fig. 2. SNR ratio variation with microcalcification thickness at 30 kV using two different anode materials.

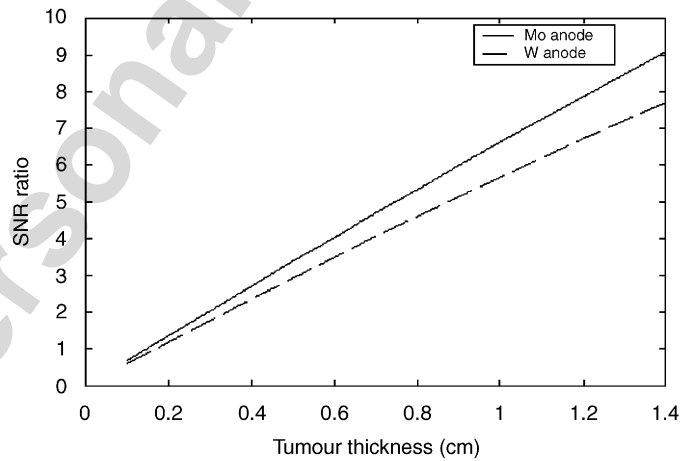


Fig. 3. SNR ratio variation with tumor thickness at 30 kV using two different anode materials molybdenum and tungsten.

Table 1
SNR for software breast phantom with 50% adipose and 50% glandular, GOS scintillator material and cosine reconstruction filter

X-ray tube voltage (kV)	Calcification		Carcinoma	
	Non-energy-weighted technique	Energy-weighted technique	Non-energy-weighted technique	Energy-weighted technique
20	14.49	15.94	3.5	3.9
25	12.61	13.24	4.2	4.49
30	10.44	11.27	3.50	3.59
35	9.55	10.13	3.11	3.36
40	9.00	9.90	2.62	2.86

enhancement effect is more significant, which is in agreement with previous reports [1]. In the case that a tumor is present, again the SNR is enhanced by a factor that can reach values up to 9.07 for tumor sizes of 0.2 and 1.4 cm, respectively. As in the previous case, the $\text{SNR}_{\text{ratio}}$ for a Mo anode is higher than for W. The reason for this is

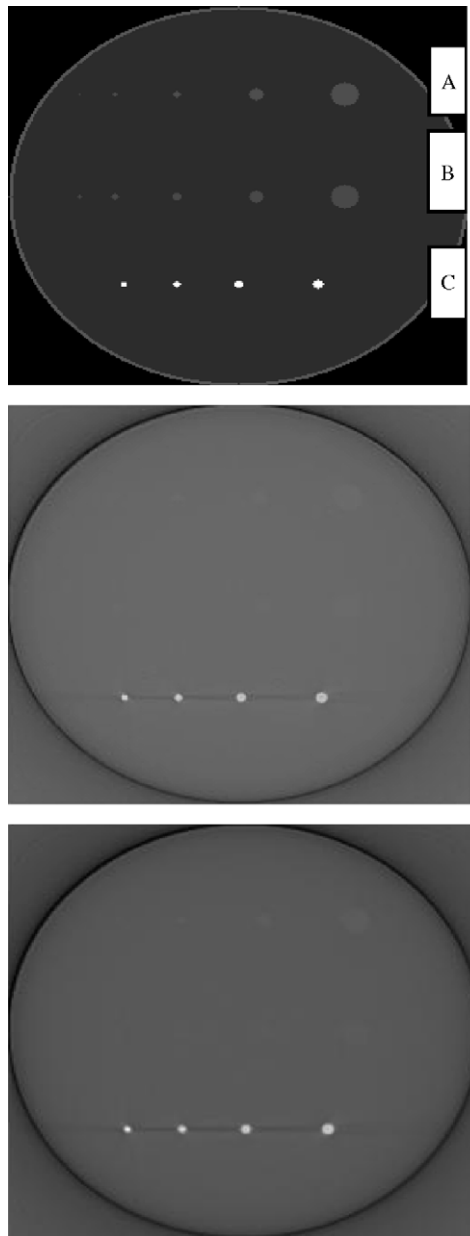


Fig. 4. Transverse image of software breast phantom with a set of objects and base material with 50% adipose and 50% glandular (upper) with linear attenuation coefficients for 4 keV. A: glandular objects (upper row, 0.5, 1, 2, 4 and 8 mm from left to right), B: carcinomas (middle row, 1, 2, 2.5, 4 and 8 mm) and C: calcifications (bottom row, 1.5, 2, 2.5 and 3 mm). Reconstructed CTBI with non-energy-weighted (middle) and energy-weighted (bottom) technique for X-ray spectrum of 20 kV.

that the Mo spectrum shows stronger variation with respect to energy, leading to larger weighting factor and SNR enhancement, as it has been previously reported by other studies [1].

The factor of enhancement is greater when microcalcification is present. This is due to the difference in the attenuation coefficients of the two regions. In the same

energy interval (3.5–10.5 keV), the microcalcification attenuation coefficient μ is many orders of magnitude greater than that of the tumor.

Moreover, the energy-weighting technique produced images with higher SNR for both software phantoms than non-energy-weighted technique. Table 1 shows the SNR increase with the energy-weighted technique for every studied anatomical structure, verifying the previous results. In terms of scintillator-detector materials the Hilgrit and GOS were performed equally well, while the Cosine filter produced images with higher SNR than other filters. Furthermore, SNR increased in both studied phantoms applying the energy-weighted technique (Fig. 4).

6. Conclusions

The purpose of this study was to investigate how the energy-weighting technique influences the quality of SNR in typical mammographic conditions. A theoretical model was developed to simulate the X-ray imaging conditions. Results showed that SNR enhancement is achievable under such conditions. The SNR ratio of the weighted signal to the original signal can reach values up to 30. Larger enhancement is achieved when using molybdenum than tungsten spectra. In addition, microcalcification regions can lead to bigger SNR ratios than tumor regions due to the difference in the emitted signals from different regions. Such difference does exist and is particularly large in the low-energy region.

Acknowledgment

This work was financially supported by the TEI of Athens research program ‘ATHINA 2004’.

References

- [1] R.N. Cahn, B. Cederström, M. Danielsson, A. Hall, M. Lundqvist, D. Nygren, *Med. Phys.* 26 (1999) 2680.
- [2] J. Griesh, D. Niederlöhner, G. Anton, *Nucl. Instr. and Meth. A* 531 (2004) 68.
- [3] C.W.E. Van Eijk, *Phys. Med. Biol.* 47 (2002) R85.
- [4] <http://www.med.siemens.com/med/rv/spektrum/mamIn.asp>.
- [5] J.M. Boone, T.R. Fewell, R.J. Jennings, *Med. Phys.* 24 (12) (1997) 1863.
- [6] G.W. Ludwig, *J. Electrochem. Soc.* 118 (1971) 1152.
- [7] R.K. Swank, *Appl. Opt.* 12 (1973) 1865.
- [8] J. Beutel, B.A. Apple, R. Shaw, *Phys. Med. Biol.* 38 (1993) 1181.
- [9] I. Kandarakis, D. Cavouras, G.S. Panayiotakis, C.D. Nomicos, *Phys. Med. Biol.* 42 (1997) 1351.
- [10] I. Kandarakis, et al., *Nucl. Instr. and Meth. B* 179 (2001) 215.
- [11] A. Gaitanis, I. Kandarakis, et al., in: *Biomedizinische Technik/ Medical Physics Proceedings, 14th International Conference of Medical Physics*, vol. 50, Supplementary vol. 1, Part 1, 2005, pp. 354–355.
- [12] B. Chen, R. Ning, *Med. Phys.* 29 (5) (2002) 755.